

This leads to a reduction of the threshold voltage  $V_T$  resulting in an increase of the drain current, the so called 'kink effect' [8]. This effect is easily observed in the experimental drain and bulk currents plotted in Fig. 4. If the temperature dependence of the bulk impedance is incorporated into the model, the multiplication factor may be predicted for temperatures below  $T_{cf}$ , thus allowing us to predict the related kink effect.

**Conclusions:** The characterisation of the carrier multiplication  $M$  of submicrometre pMOS transistors, over the temperature range of 30–300 K for different bias conditions, is reported. Additionally it has been demonstrated that by means of the already existing models,  $M$  can be predicted from room temperature down to the critical temperature  $T_{cf}$ . Below  $T_{cf}$  the incorporation of the bulk impedance into the model may serve to predict  $M$  down to 4–2 K. The three regions experimentally observed in the  $M$ – $T$  characteristics have been explained in terms of the bias and temperature dependence of the mean free path. Furthermore by using the model, the influence of the technology on the  $M$ – $T$  characteristics, as are  $\partial M/\partial T$  in the linear region, and the critical temperatures  $T_{cs}$  and  $T_{cf}$  in the saturation region, can be investigated.

21st October 1991

E. A. Gutiérrez-D.,\* L. Deferm and G. Declerck (IMEC, Kapeldreef 75, B-3001, Leuven, Belgium)

\* On leave from the National Institute of Astrophysics, Optics and Electronics (INAOE), Puebla, México, and partially supported by CONACYT-México.

## References

- DEEN, M. J., and WANG, J.: 'Substrate currents in short buried-channel PMOS devices at cryogenic temperatures', *Cryogenics*, 1990, **30**, pp. 1113–1117
- HENNING, K. A., CHAN, N., and PLUMMER, J. D.: 'Substrate current in n-channel and p-channel MOSFETs between 77 and 300 K: characterization and simulation', *IEDM*, 1985, pp. 573–576
- HWANG, C. G., and DUTTON, R. W.: 'Substrate current model for submicrometer MOSFETs based on mean free path', *IEEE Trans.*, 1989, **ED-36**, pp. 1348–1354
- JACOBONI, C., CANALI, C., OTTAVIANI, G., and QUARANTA, A.: 'A review of some charge transport properties of silicon', *Solid-State Electron.*, 1977, **20**, pp. 77–89
- ARORA, N. D., and SHARMA, M. S.: 'MOSFET substrate current model for circuit simulation', *IEEE Trans.*, 1991, **ED-38**, pp. 1392–1398
- TANG, J. Y., and HESS, K.: 'Impact ionization of electrons in silicon (steady state)', *J. Appl. Phys.*, 1983, **54**, pp. 5139–5144
- CROWELL, C. R., and SZE, S. M.: 'Temperature dependence of avalanche multiplication in semiconductors', *Appl. Phys. Lett.*, 1966, **9**, pp. 242–244
- SMOEN, E., DEFERM, L., and CLAEYS, C.: 'Analytical model for the kink in nMOSTs operating at liquid helium temperatures (LHT)', *Solid-State Electron.*, 1990, **33**, pp. 445–454

## DESIGN OF IIR DIGITAL FILTERS USING COMPLEX ALLPASS NETWORK BASED ON EIGENVALUE PROBLEM

X. Zhang and H. Iwakura

*Indexing terms: Digital filters, Filters*

A new design method is presented for complementary IIR digital filters with given magnitude specifications based on the eigenvalue problem, which are composed of a single complex allpass section.

**Introduction:** It is well known that a class of odd- and even-order complementary IIR digital filters [1] can be constructed by using a parallel interconnection of two allpass sections with real and complex conjugate coefficients. Many design procedures [2–4] for this class of filter have been presented,

however these approaches have not succeeded in obtaining the optimal filter parameters with the desired magnitude specifications.

The purpose of this Letter is to develop a new method for designing even order IIR digital filters with given magnitude specifications using a single complex allpass section. The design procedure is based on the formulation of an eigenvalue problem which relates the filter coefficients with the magnitude errors in the specified frequency range; the optimal filter coefficients are obtained by computing the maximum eigenvector and applying an iteration procedure.

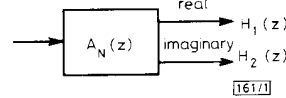


Fig. 1 IIR digital filters using complex allpass section

**IIR digital filters using complex allpass section:** The even order IIR digital filters, composed of a parallel interconnection of two allpass sections with conjugate complex coefficients, can be obtained by implementing a single complex allpass section as shown in Fig. 1. The transfer functions  $H_1(z)$ ,  $H_2(z)$  are given by

$$H_1(z) = \frac{1}{2}[A_N(z) + A_N^*(z)] = \text{Re}\{A_N(z)\} \quad (1)$$

$$H_2(z) = \frac{1}{2j}[A_N(z) - A_N^*(z)] = \text{Im}\{A_N(z)\} \quad (2)$$

where  $A_N(z)$  is an  $N$ th-order stable complex allpass function, and  $A_N^*(z)$  is a conjugate pair of  $A_N(z)$ . The transfer function  $A_N(z)$  is defined as follows:

$$A_N(z) = z^{-N} \frac{\sum_{n=0}^N a_n^* z^n}{\sum_{n=0}^N a_n z^{-n}} \quad (3)$$

where  $a_n$  are complex and  $a_n^*$  are complex conjugates of  $a_n$ .

The transfer function  $H_1(z)$  of eqn. 1 can be rewritten as

$$H_1(z) = \frac{1}{2}A_N^*(z)[G(z) + 1] \quad (4)$$

where

$$G(z) = \frac{A_N(z)}{A_N^*(z)} = \frac{\sum_{n=-N}^N g_n^* z^n}{\sum_{n=-N}^N g_n z^n} \quad (5)$$

$$g_n = g_{-n} = g_{nr} + jg_{ni} \quad (6)$$

It is clear from eqn. 5 that  $G(z)$  is an unstable allpass function. However, we assume that the poles of  $G(z)$  located inside the unit circle are  $z_k$ , the roots  $1/z_k^*$  are also poles of  $G(z)$  because of the condition  $g_n = g_{-n}$ , and its corresponding zeros are  $z_k^*$ ,  $1/z_k^*$ , respectively. We can reconstruct a stable allpass function  $A_N(z)[A_N^*(z)]$  by using poles  $z_k(z_k^*)$  and zeros  $1/z_k^*(1/z_k)$ ; then the stable transfer functions  $H_1(z)$ ,  $H_2(z)$  can be obtained. From eqn. 5, we have

$$G(e^{j\omega}) = e^{-j2\varphi} \quad (7)$$

$$\varphi = \tan^{-1} \frac{\frac{g_{0i}}{2} + \sum_{n=1}^N g_{ni} \cos n\omega}{\frac{g_{0r}}{2} + \sum_{n=1}^N g_{nr} \cos n\omega} \quad (8)$$

where  $2\varphi$  is the phase difference between  $A_N(z)$  and  $A_N^*(z)$ , and is also the phase characteristic of  $G(z)$ .

**Formulation based on eigenvalue problem:** Let us consider the design problem of a complementary pair of a lowpass filter (LPF) and highpass filter (HPF). From eqn. 4, the magnitude response of  $H_1(z)$  is determined only by the performance of  $G(z)$ . Therefore, the design problem for this class of filter now becomes that of how to design the phase characteristic of  $G(z)$ . The phase of  $G(z)$  has to be 0 ( $\varphi = 0$ ) in the passband, and  $\pm\pi$  ( $\varphi = \mp\pi/2$ ) in the stopband.

To solve this problem we use the Remez exchange algorithm, and formulate the condition for  $\varphi$  in the form of an eigenvalue problem. By selecting extremal frequencies  $\omega_{ip}$ ,  $\omega_{is}$  ( $i = 0, 1, \dots, N$ ) in the passband and stopband [4], we want to find filter coefficients  $g_n$  that satisfy the following conditions:

$$\frac{g_{0i}}{2} + \sum_{n=1}^N g_{ni} \cos n\omega_{ip} = (-1)^i \tan \varphi_p$$

$$\frac{g_{0r}}{2} + \sum_{n=1}^N g_{nr} \cos n\omega_{ip} = (-1)^i \delta_p \quad (9)$$

$$\frac{g_{0r}}{2} + \sum_{n=1}^N g_{nr} \cos n\omega_{is} = (-1)^i \cot \left( \varphi_s + \frac{\pi}{2} \right)$$

$$\frac{g_{0i}}{2} + \sum_{n=1}^N g_{ni} \cos n\omega_{is} = (-1)^i \delta_s \quad (10)$$

where

$$\omega_{cp} = \omega_{0p} > \omega_{1p} > \dots > \omega_{(N-1)p} > \omega_{Np} = 0 \quad (11)$$

$$\omega_{cs} = \omega_{0s} < \omega_{1s} < \dots < \omega_{(N-1)s} < \omega_{Ns} = \pi \quad (12)$$

In general, the phase deviations ( $\varphi_p$ ,  $\varphi_s$ ) from its ideal values will be very small, then

$$\varphi_p = \tan^{-1} \delta_p \simeq \delta_p \quad \varphi_s = \tan^{-1} \delta_s \simeq \delta_s \quad (13)$$

We can rewrite eqns. 9 and 10 in matrix form as

$$\mathbf{P}_p \mathbf{G}_i = \delta_p \mathbf{Q}_p \mathbf{G}_r \quad (14)$$

$$\mathbf{P}_s \mathbf{G}_r = \delta_s \mathbf{Q}_s \mathbf{G}_i \quad (15)$$

where

$$\mathbf{G}_i = [g_{0i}, g_{1i}, \dots, g_{Ni}]^T \quad (16)$$

$$\mathbf{G}_r = [g_{0r}, g_{1r}, \dots, g_{Nr}]^T \quad (17)$$

The elements of the matrix  $\mathbf{P}_p$ ,  $\mathbf{P}_s$ ,  $\mathbf{Q}_p$ ,  $\mathbf{Q}_s$  are given by

$$\begin{cases} P_{pij} \\ P_{sij} \end{cases} = \begin{cases} 0.5 & (j=0) \\ \cos j\omega_{ip} & (j=1, 2, \dots, N) \end{cases} \quad (18)$$

$$\begin{cases} Q_{pij} \\ Q_{sij} \end{cases} = \begin{cases} (-1)^j 0.5 & (j=0) \\ (-1)^j \cos j\omega_{ip} & (j=1, 2, \dots, N) \end{cases} \quad (19)$$

Because  $\mathbf{P}_p$ ,  $\mathbf{P}_s$  are nonsingular matrices [4], by eliminating  $\mathbf{G}_i$  from eqns. 14 and 15, we obtain

$$\lambda \mathbf{G}_r = \mathbf{T} \mathbf{G}_r \quad (20)$$

where

$$\lambda = \frac{1}{\delta_p \delta_s} \quad (21)$$

$$\mathbf{T} = \mathbf{P}_s^{-1} \mathbf{Q}_s \mathbf{P}_p^{-1} \mathbf{Q}_p \quad (22)$$

It should be noted that eqn. 20 corresponds to an eigenvalue problem. The eigenvalue is expressed in eqn. 21 as a product of  $\delta_p \delta_s (\lambda = \lambda^{-1})$ . Therefore, one of the errors  $\delta_p$ ,  $\delta_s$  can be arbitrarily given. As an example, assuming that  $\delta_s$  is specified, the optimal solution is given by minimising the error  $\delta_p$ . Thus, the maximum eigenvalue  $\lambda_M$  gives the minimum error  $\delta_{pmin}$ , and the corresponding maximum eigenvector  $\mathbf{G}_r$  gives the real parts  $g_{nr}$  of filter coefficients. From eqn. 14 or 15, the imaginary parts  $g_{ni}$  of filter coefficients can be found, and the transfer function  $H_1(z)$  is determined by using the filter coefficients  $g_n$ .

Next, searching the peak frequency points of  $\varphi$  in all frequency range, and replacing the extremal frequency points  $\omega_{ip(s)}$  by the obtained peak frequencies  $\Omega_{ip(s)}$ , we repeat the computation until the optimal filter coefficients  $g_n$  are obtained.

Let  $\Delta_{Lp}$ ,  $\Delta_{Ls}$ ,  $\Delta_{Hp}$  and  $\Delta_{Hs}$  be the passband and stopband ripple of magnitudes of  $H_1(z)$  and  $H_2(z)$ , respectively. Using  $\varphi_p$ ,  $\varphi_s$  and  $\delta_p$ ,  $\delta_s$ , these ripples are given by

$$\Delta_{Lp} = 1 - \cos \varphi_p \simeq \frac{1}{2} \delta_p^2 \quad \Delta_{Ls} = \sin \varphi_s \simeq \delta_s$$

$$\Delta_{Hp} = 1 - \cos \varphi_s \simeq \frac{1}{2} \delta_s^2 \quad \Delta_{Hs} = \sin \varphi_p \simeq \delta_p \quad (23)$$

Thus, if one of the passband or stopband magnitude ripples of the filters is given, then  $\delta_p$  or  $\delta_s$  can be determined.

As a result, the optimal filters with given magnitude specifications, and also equiripple magnitude response, can be designed by this approach.

**Design algorithm:**

**procedure** {design algorithm of IIR digital filters}  
**begin**

(1) read  $N$ ,  $\omega_{cp}$ ,  $\omega_{cs}$ , and the magnitude ripple specification in the passband or stopband

(2) select initial passband and stopband extremal frequencies  $\Omega_{ip}(\omega_{cp} = \Omega_{0p} > \Omega_{1p} > \dots > \Omega_{Np} = 0)$ ,  $\Omega_{is}(\omega_{cs} = \Omega_{0s} < \Omega_{1s} < \dots < \Omega_{Ns} = \pi)$  equally spaced in the frequency range  $[0, \omega_{cp}]$ ,  $[\omega_{cs}, \pi]$ .

**repeat**

(3) set  $\omega_{ip} = \Omega_{ip}$  and  $\omega_{is} = \Omega_{is}$  (for  $i = 0, 1, \dots, N$ )

(4) compute  $\mathbf{P}_p$ ,  $\mathbf{Q}_p$ ,  $\mathbf{P}_s$  and  $\mathbf{Q}_s$  by using eqns. 18, 19, and find the maximum eigenvector of  $\mathbf{P}_s^{-1} \mathbf{Q}_s \mathbf{P}_p^{-1} \mathbf{Q}_p$  to obtain the real parts  $g_{nr}$  of the filter coefficients

(5) find the imaginary parts  $g_{ni}$  from eqn. 14 or 15 using  $\delta_p$  or  $\delta_s$  which are obtained from the given magnitude specification; then determine the complex allpass function  $A_N(z)$

(6) search the peak frequency points of  $\varphi$ , and store them into the corresponding  $\Omega_{ip}$ ,  $\Omega_{is}$

**until** satisfy the following conditions for prescribed small constants  $\varepsilon_1$ ,  $\varepsilon_2$ :

$$|\Omega_{ip} - \omega_{ip}| \leq \varepsilon_1 \quad |\Omega_{is} - \omega_{is}| \leq \varepsilon_2 \quad (\text{for } i = 0, 1, \dots, N)$$

**end.**

**Design examples:** The aim is to design a complementary pair of an LPF and HPF with the following specifications:  $N = 4$ , passband  $f/f_s: 0.0-0.15$ , stopband  $f/f_s: 0.2-0.5$ .

The magnitude responses of designed LPF and HPF pair with the specification  $K_s = \Delta_{Ls}/\Delta_{Hs} = 1$  are shown in Fig. 2 by

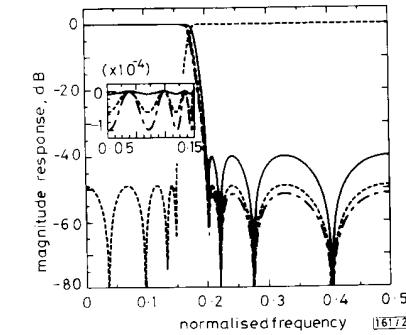


**Fig. 2** Magnitude responses of LPF

—  $L_s = 40$  (dB)  
---  $K_s = 1$   
- · -  $L_p = 10^{-4}$  (dB)

using dotted lines. The magnitude response with stopband attenuation  $L_s = 40$  dB ( $\Delta L_s = 0.01$ ), and that with the passband attenuation  $L_p = 10^{-4}$  dB ( $\Delta L_p = 1.15 \times 10^{-5}$ ) are also shown in Fig. 2. The number of iterations required for converging to equiripple characteristics is about 4 to 5.

**Conclusion:** We have proposed a new design method for IIR digital filters using a complex allpass network based on the eigenvalue problem. By using the Remez exchange algorithm, and giving the specified error magnitudes, we formulate the phase difference between a conjugate pair of complex allpass sections in the form of an eigenvalue problem. We can then obtain the optimal filter coefficients by computing the maximum eigenvector and applying an iteration procedure. The main feature of this method is that the magnitude ripple in the passband or stopband of filters can be arbitrarily specified and the optimal solution can be easily obtained.

28th October 1991

X. Zhang and H. Iwakura (Faculty of Electro-Communication, The University of Electro-Communications, Chofu-shi, 182 Tokyo, Japan)

## References

1. VAIDYANATHAN, P. P., REGALIA, P. A., and MITRA, S. K.: 'Design of doubly-complementary IIR digital filters using a single complex allpass filter, with multirate applications', *IEEE Trans.*, 1987, **CAS-34**, pp. 378-389
2. ANSARI, R., and LIU, B.: 'A class of low-noise computationally efficient recursive digital filters with applications to sampling rate alterations', *IEEE Trans.*, 1985, **ASSP-33**, pp. 90-97
3. IKEYAMA, M., INOUE, H., TOYOSHIMA, H., and TAKAHASHI, S.: 'Design of IIR digital quadrature mirror filters based on an analog filter theory', *Trans. IEICE, Japan*, 1990, **J73-A**, pp. 801-808 (in Japanese)
4. ZHANG, X., and IWAKURA, H.: 'Design of complementary IIR digital filters using allpass networks'. IEICE Technical Reports of Japan, 1991, **CAS91-35**, pp. 43-50 (in Japanese)

## INPUT VOLTAGE SENSITIVITY OF GaAs/GaAlAs HEMT LATCHED COMPARATOR

S. Feng and D. Seitzer

**Indexing terms:** Circuit theory and design, Comparators, Gallium arsenide

The input voltage sensitivity represents a critical parameter for a latched comparator in high-speed and high-precision data conversion applications. An analytical prediction of this parameter is presented and it has been verified to be in good agreement with the experimental results from a high performance latched comparator implemented in 0.5  $\mu$ m GaAs/GaAlAs E/D HEMT technology.

**Introduction:** The latched voltage comparator with a broadband preamplifier and a regenerative latch in fully differential form in Fig. 1 has been widely used in high-speed and high-

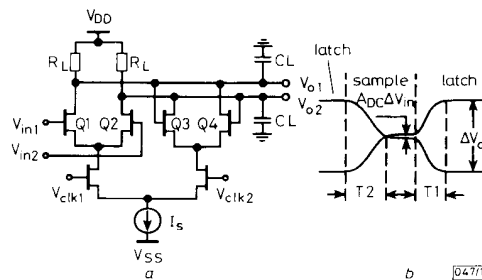


Fig. 1 Simple latched comparator and output waveforms

- a Latched comparator
- b Output waveforms

precision analogue-to-digital and digital-to-analogue converters (ADCs and DACs). An important parameter for the circuit is the input voltage sensitivity, which is defined as the critical input voltage that the circuit can resolve at a given clock frequency. This parameter should be a function of DC input offset voltage, input and clock signal frequencies, parasitic capacitance, load impedance and power dissipation. In GaAs technologies, the input voltage sensitivity of the latched comparators has been demonstrated experimentally to be 1-2 mV at 1.0 Gbit/s, 8-10 mV at 4.0 Gbit/s and 30 mV at 8.0 Gbit/s [1-3]. However, there is no suitable analytical analysis of the parameter for GaAs comparators. This Letter discusses an analytical method for the input voltage sensitivity based on linearised equivalent circuit models, and an identical result has been achieved between the prediction and measurement on an implemented GaAs/GaAlAs HEMT latched comparator.

**Circuit configuration:** As shown in Fig. 2, the circuit consists of an input amplifier and two simple latched comparators of Fig. 1 in cascade (LCOMP1 and LCOMP2) as master-slave flipflops, in which the source followers provide interface and level shift functions. Owing to the additional input amplifier, the switched effect in the preamplifier of the simple latched comparator is avoided and the input voltage sensitivity is improved. LCOMP2 is used as a slave flipflop for the benefit of the following encode logic in an ADC and the switched-weighted network in a DAC. This circuit has been implemented in the 0.5  $\mu$ m GaAs/GaAlAs E/D HEMT technology of the Fraunhofer-Institute for Applied Solid-State Physics, Germany. The HSPICE model parameters of the E/D HEMTs can be found in Reference 2.

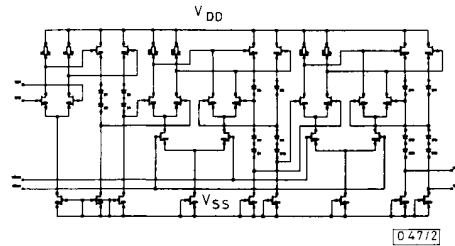


Fig. 2 Latched comparator implemented in 0.5  $\mu$ m E/D HEMT technology

**Analytical prediction:** The calculation of the regeneration time  $T1$  and recovery time  $T2$  of the simple latched comparator in Fig. 1 using linearised equivalent circuit models in silicon technology has been discussed [4, 5]. In a GaAs FET (MESFET or HEMT) circuit, the sample and latch modes will be described by the models in Fig. 3a and b, respectively. The equivalent elements from the differential pair Q3, Q4 are designated by subscript 2. Solving the circuit equations at nodes  $V_{01}$  and  $V_{02}$ , the output response  $V_{01}-V_{02}$  is described

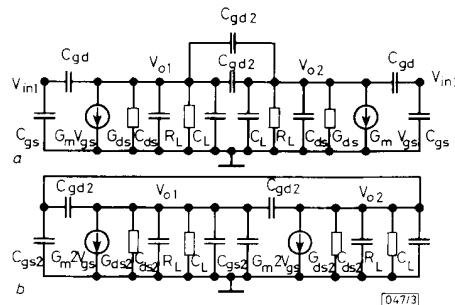


Fig. 3 Linearised equivalent circuit models of GaAs FET latched comparator

- a Sample mode
- b Latch mode